



# Research & Reviews On

# Electrochemistry

Full Paper

RREC, 5(5), 2014 [142-148]

## Natural and chemically synthesized DSSC efficiency upgrading using silver nitrate additive

Wesam A.A.Twej\*<sup>1</sup>, Mohanad M.Azzawi<sup>2</sup>, A.S.Hasaani<sup>1</sup>, Dheyaa B.Alwan<sup>1</sup>

<sup>1</sup>Physics Department, College of Science, University of Baghdad, Al-Jadiriya, Baghdad, (IRAQ)

<sup>2</sup>Ministry of science and technology, (IRAQ)

E-mail : wesam961@yahoo.co.in

### ABSTRACT

This work reports on a method concerning the improvement of the performance of chemically synthesized and natural dye-sensitized nanocrystalline TiO<sub>2</sub> solar cells efficiency. This method deals with adding surface passivation elements to the electrolyte. Ruthenium N719 is used as chemically synthesized dye, while pomegranate juice as well as several fruit juice as neutral dyes. The dependence of the efficiency on the additives has been discussed. It is found that the addition of 1 g / L AgNO<sub>3</sub> to the electrolyte solution in Ruthenium N719 DSSC resulted in nearly doubling the short circuit current and overall light to electricity conversion efficiency with slight increase in the open circuit voltage and fill factor. Moreover, in the case of natural cells, this addition nearly doubles the fill factor, maximum circuit voltage and conversion efficiency and has no effect on the circuit current. The addition of AgNO<sub>3</sub> to Ruthenium cell under an illumination of 40 mW/cm<sup>2</sup> sun simulator exhibits good photovoltaic performance; the efficiency reaches 3.7% (5.3 mA cm<sup>-2</sup> J<sub>sc</sub>, 680 mV V<sub>oc</sub>, and 69 % fill factor). This additive accomplished enhancing in the upgraded DSSC efficiency from 1.9 % to 3.7 %. © 2014 Trade Science Inc. - INDIA

### KEYWORDS

DSSC;  
TiO<sub>2</sub>;  
Efficiency;  
AgNO<sub>3</sub> additive.

### INTRODUCTION

During the last few decades, there have been intensive research activities to explore green sources of energy<sup>[1-6]</sup>. An alternative solar cell technology is the dye-sensitized solar cell (DSSC) also known as Grätzel cell<sup>[3]</sup>, which is characterized as lightweight, portable, inexpensive, and transparent relative to conventional solid state solar cells<sup>[7]</sup>. Hence, most studies on DSSC are intended to understand the prevailing role of elec-

tron transfer dynamics and kinetics at nanocrystalline metal oxide/sensitizer dye/electrolyte interfaces<sup>[8]</sup>. The Natural (DSSC's) are among the most promising devices for the solar energy conversion due to their low production cost and low environmental impact<sup>[3]</sup>. DSSCs exhibit a range of interesting features as adequately inexpensive renewable energy sources<sup>[4,9]</sup>. The structure of a DSSC is made of three main parts; counter electrode, photo anode and an electrolyte. Counter electrode, normally conductive glass and a fluorine-

doped tin oxide (FTO) the most commonly used, coated with few atomic layers of carbon or platinum, in order to catalyse the red-ox reaction with the electrolyte<sup>[10-12]</sup>. Photo anode is constructed from semiconductor oxide porous film on a conductive glass substrate anchored a monolayer of dye. The electrolyte can be made from organic solvent containing a red-ox couple such as iodide/tri-iodide.

The quality and anchoring of the dye to the surface of semiconductor oxide porous film are important processes determining the photo conversion efficiency PCE of the cell<sup>[10]</sup>. The huge mesoporous surface allows for an adsorption of a sufficiently large number of dye molecules for efficient light harvesting<sup>[10,11]</sup>.

In the DSSCs, the open circuit voltage ( $V_{oc}$ ) is dictated by the difference between the quasi-Fermi level of the  $TiO_2$  and the potential of the redox couple, while the short circuit current ( $J_{sc}$ ) arises by the efficiencies of the electron injection from the dye into  $TiO_2$  and charge collection. Therefore, both values are limited by the recombination processes<sup>[13]</sup> that occur when the photoinjected electron recombines with the oxidized dye molecule or reacts with the oxidized form of the redox couple in the electrolyte. The second process has been well-studied<sup>[14]</sup> and deemed to have a greater impact on device performance than the second one.

The efficiency limitation of the DSSCs is considered as a big challenge to be in a widespread commercial application. Various strategies are being employed to overcome such intrinsic limitation<sup>[15]</sup>.

In addition to a redox couple, two types of additives are normally introduced into the liquid electrolytes. Specific alkali organidiumcations and Nitrogen-containing heterocyclic compounds such as 4-tert-butylpyridine (4-TBP) and Derivatives of N-alkylbenzimidazole. The first type is mainly devoted to the enhancement of ( $J_{sc}$ ), by shifting the conducting band (CB) of the  $TiO_2$  towards more positive potentials, thus affecting the electron injection dynamics of the excited state of dye molecules. The second additives type is mainly dedicated to the improvement of the  $V_{oc}$ <sup>[16-18]</sup>.

It has been found that the photovoltaic performance of DSSCs can be enhanced substantially by adding a small amount of deferent additive<sup>[19]</sup>.

The objective of this work is to discuss and investigate the  $AgNO_3$  additive enhancement of the photo-

voltaic performance of natural and chemically synthesized DSSCs.

## MATERIAL AND METHOD

### Materials

All chemicals were used without further purification unless otherwise stated.

Potassium iodide (KI), iodide (I), distilled water, ethanol, acetonitrile, FTO (7 Ohm/sq) transmission (80%) and N719 stands for di-tetrabutylammoniumcis-bis (isothiocyanato) bis (2,22 -bipyridyl-4,42 -dicarboxylato) ruthenium complex both supplied by [Solaronix].  $TiO_2$  nanocrystalline (anatase 10 nm) purity (99.9%) was supplied by [MK nano – Canada].

The fruits from which the natural dyes were extracted are listed in TABLE 1.

TABLE 1 : The origin of the neutral dyes

Type of plant	Origin
Pomegranate	Iraq
Hibiscus sabdrifol	Egypt
Raspberry	Syrian
Red orange	Iran
Grapefruit	Indian
Black tea	Sri lanka
Borago officinalis	Egypt

### Preparation

The preparation procedure is described in ref.<sup>[20]</sup>. However, an addition in this work was the dissolving of definite amounts of  $AgNO_3$  in 10 ml of acetonitrile. This solution was added to (KI, I) solution under RT stirrer. A drop of the resulting solution was injected on the edge of the cells.

The area of all sensitized films was fixed to 1  $cm^2$  using a tape of 17  $\mu m$  thick as a mask for this purpose and by doing so all prepared  $TiO_2$  paste films were kept unchanged at 17  $\mu m$ . The illumination was performed by, sun simulator, mercury tungsten blended lamp (Robium-D) China. During measurements, the irradiance on the cells was fixed at 40  $mW/cm^2$ .

### DSSC performance

Photo response of the DSSC was evaluated by

## Full Paper

recording the I-V characteristics with a  $500\ \Omega$  potentiometer as a variable load as shown in Figure 1.

Here,  $S_1$  and  $S_2$  are two electrical switches used for open circuit and close circuit measurements. Both of them should be opened to measure  $V_{oc}$ , while  $S_1$  should be open and  $S_2$  closed to measure  $I_{sc}$ . In the case of normal operation,  $S_1$  should be opened and  $S_2$  is closed.

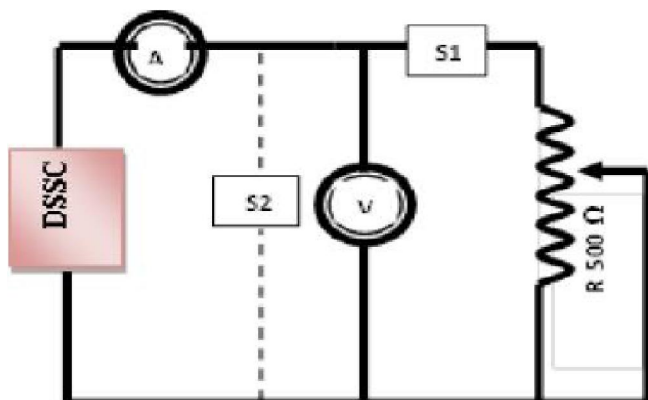


Figure 1 : Electrical circuit diagram adapted for measuring the I-V characteristics

## RESULTS

In order to investigate the absorption band of the selected dyes in the interesting solar spectral region, the UV-VIS absorption spectra ought to be recorded for these dyes. These UV-VIS absorption spectra of these dyes are shown in Figure 2.

Figure 2 (a-d) shows the absorption spectra of four natural dyes. These dyes have notable colors in the visible region, but they have only spectral UV absorption bands and no significant absorption bands in the visible region. However, there are tails of their UV absorption bands that can be weakly considered in sensitizing processes. Regard to Figure 2 (e and f) it is found that rather than the UV peaks, there are other absorption peaks at about (520 nm) and (535 nm) that belong to pomegranate juice and Ruthenium N719 dye respectively. The positions of these peaks are in a good matching with the peak of the visible solar radiation spectrum. Therefore, these two dyes were expected effectively as good promising dyes.

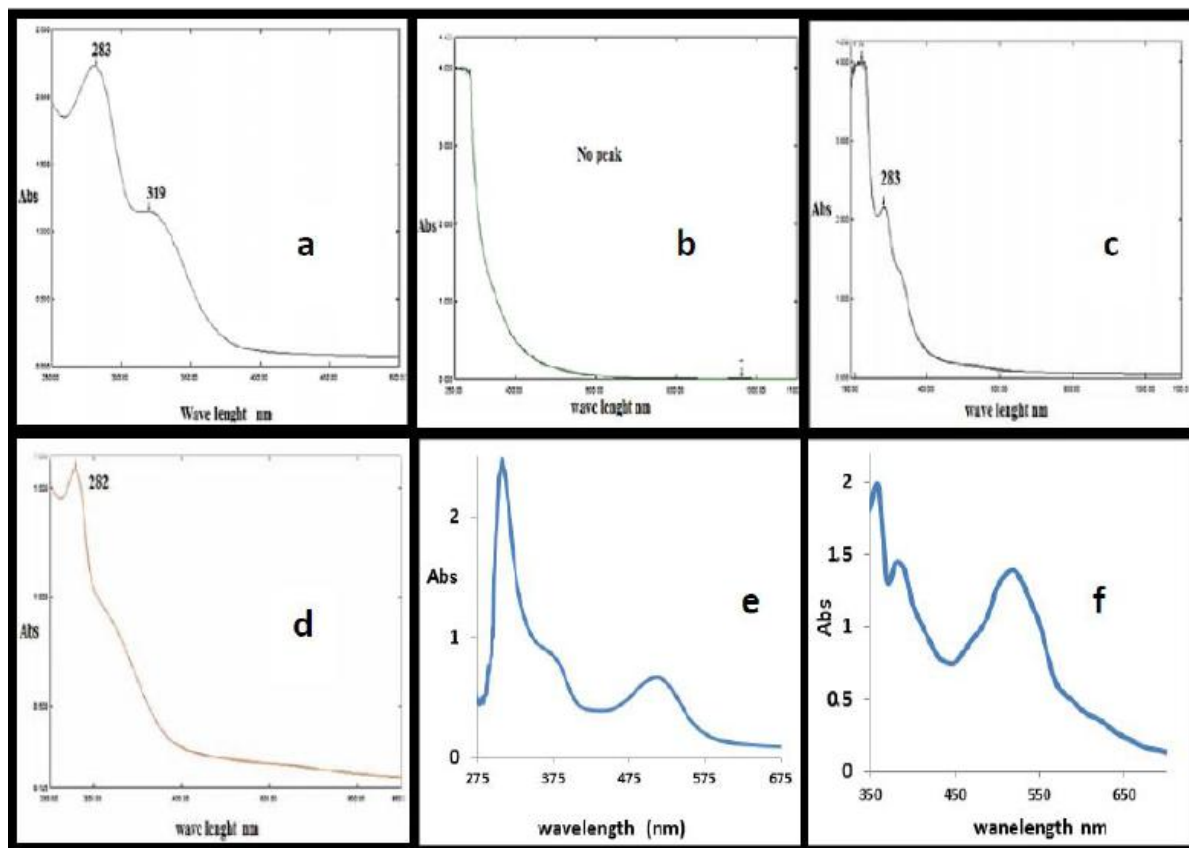
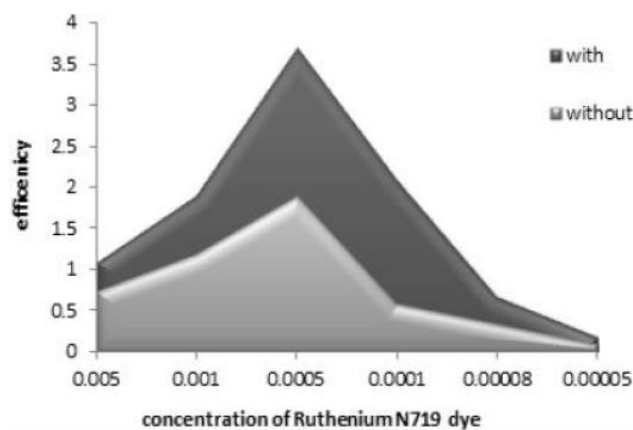


Figure 2 : Absorption spectra for (a) Hibiscus sabdrifol (b) Grapefruit (c) Borago officinalis (d) Black tea (e) diluted pomegranate juice (f) ruthenium N719 dye.

TABLE 2 : DSSC performance before and after the addition of AgNO<sub>3</sub>

Dye type	Process	I <sub>sc</sub> mA	V <sub>oc</sub> V	I <sub>max</sub> mA	V <sub>max</sub> V	FF	η %
Ruthenium	before	3.2	0.52	2.2	0.46	0.61	1.95
	after	5.3	0.68	4.29	0.58	0.69	3.7 %
Pomegranate	before	1.3	0.55	1.1	0.2	0.31	0.55 %
	after	1.3	0.7	1.2	0.4	0.53	1.2 %
Hibiscus sabdriffol	before	0.56	0.54	0.45	0.23	0.34	0.26 %
	after	0.6	0.35	0.5	0.3	0.71	0.4 %
Raspberry	before	0.7	0.52	0.59	0.2	0.32	0.3 %
	after	0.75	0.5	0.7	0.2	0.37	0.34 %
Red orange	before	0.45	0.36	0.3	0.21	0.39	0.1 %
	after	0.3	0.41	0.26	0.3	0.63	0.2 %
Grapefruit	before	0.2	0.18	0.1	0.1	0.28	0.02 %
	after	0.22	0.4	0.15	0.2	0.33	0.1 %
Black tea	before	0.111	0.3	0.090	0.1	0.14	0.0002 %
	after	0.045	0.14	0.035	0.03	0.17	0.003 %
Borago officinalis	before	0.005	0.1	0.002	0.07	0.28	0.00000 3 %
	after	0.023	0.4	0.080	0.35	0.75	0.0001 %

Figure 3 : The efficiency of the DSSC before and after the addition of 1 gm. /LAgNO<sub>3</sub> as a function of Ruthenium dye

The PCE (η) of a solar cell is given by<sup>[21]</sup>

$$\eta = \frac{P_{out}}{P_{in}} = \frac{(J_{sc} \times V_{oc})}{P_{in}} \times FF$$

$$\text{with } FF = \frac{P_{max}}{(J_{sc} \times V_{oc})} = \frac{(J_{max} \times V_{max})}{(J_{sc} \times V_{oc})},$$

where P<sub>out</sub> is the output electrical power of the device under illumination.

The current-voltage characteristics, filling factor and efficiencies of all adopted dyes in the DSSCs are listed in TABLE 2. These results were obtained before and after the addition of AgNO<sub>3</sub>.

### Concentration effect

In order to study the effect of additive concentra-

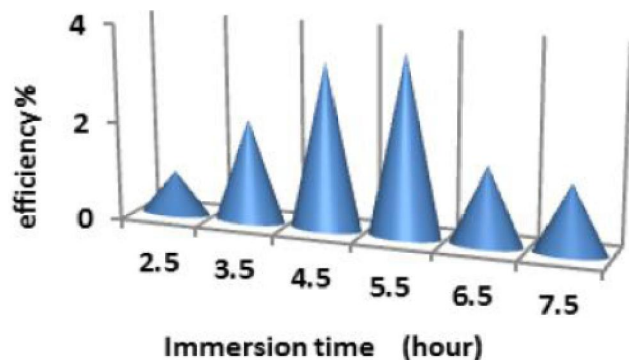


Figure 4 : Immersion time effect on the DSSC efficiency

tion on the performance of the DSSC, the effect of dye concentration had to be investigated firstly. The efficiency of the DSSC as a function of dye concentrations before and after the addition of 1 gm. /LAgNO<sub>3</sub> to the electrolyte solution is shown in Figure 3.

The prepared TiO<sub>2</sub> film after annealing process was immersed in the dye solution. Figure 4 illustrates the effect of immersion time on the DSSC efficiency.

Several metallic additives were tested in this work such as AgNO<sub>3</sub>, CuI, AuCl<sub>3</sub>, CaCO<sub>3</sub> and AuCl<sub>3</sub> +AgNO<sub>3</sub>. The final efficiency of Ruthenium N719 dye cells after the addition of the above materials are listed in TABLE 3.

From the results depicted in TABLE 3, it is obvious that AgNO<sub>3</sub> is the best solution for DSSC enhancement. The concentration of AgNO<sub>3</sub>, which was added

## Full Paper

TABLE 3 : Ruthenium DSSC efficiencies for different types of additives

type additive	$\eta$ %
AgNO <sub>3</sub>	3.7 %
CuI	1.7 %
AuCl <sub>3</sub>	1.6 %
CaCO <sub>3</sub>	1.35 %
AuCl <sub>3</sub> +AgNO <sub>3</sub>	1.06 %

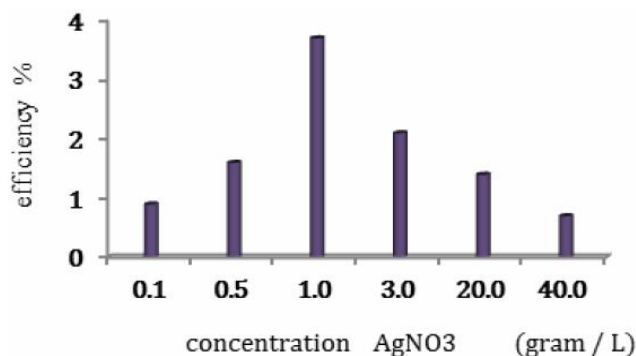


Figure 5 : Addition of AgNO<sub>3</sub> affection the DSSC efficiency to the electrolyte solution, can also affect the DSSC efficiency, providing that the suitable amount of silver nitrate is selected from Figure 5.

## DISCUSSION

The AFM images can examine the film surface morphology. The image reveals that the films average surface feature sizes are less than the grain size of 94 nm. In addition, the image discloses that all the prepared samples are compact and dense, Figure 6, before and after an annealing temperature of 723 K (450°C).

The as-deposited prepared TiO<sub>2</sub> films yield roughly nodular, while annealed films show an extra distinguished nodular morphology, which may lead to a considerable increase in the deposited film surface area. The wide surface area is favourable to give more homogenously dye distribution on the TiO<sub>2</sub> nanofilm.

Annealing temperature above 723 K (450°C) has a significant effect on the film morphology as well as more TiO<sub>2</sub> paste adhering on the substrate<sup>[21]</sup>. Therefore, it is highly recommended that the prepared TiO<sub>2</sub> films must be annealed at a temperature of 723 K (450°C) before being immersed into the sensitized dyes.

Since the dye is designated as the main effective

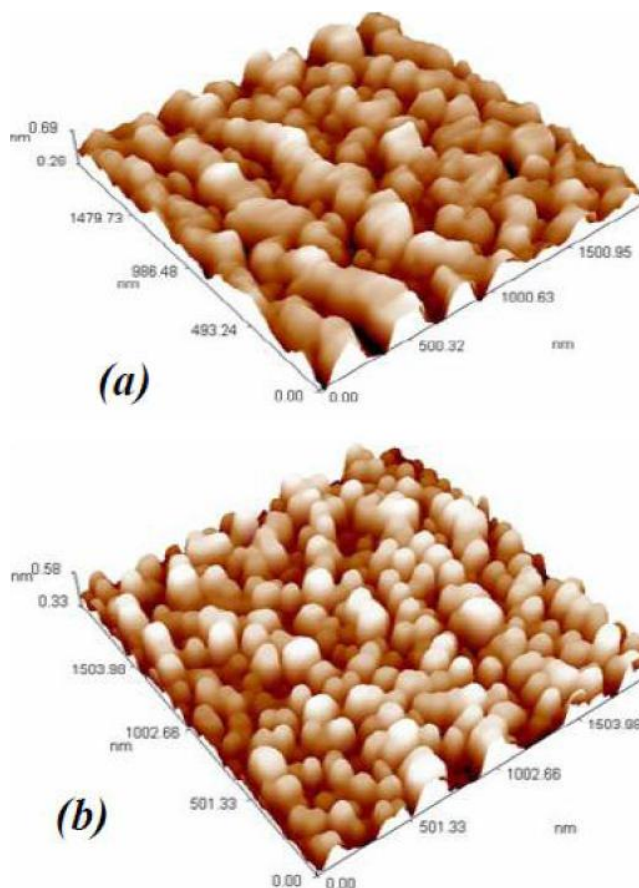


Figure 6 : The surface morphology of TiO<sub>2</sub> paste film, 3D view, (a) as deposited (b) after annealing at 723 K (450°C)

factor for charge transfer, therefore, the selected dye concentration potentially governs the DSSC performance. Throughout the present work, the Ruthenium N719 dye was found to perform the highest efficiency among all other dyes, hence, it was adopted in the concentration effect study. When a highly porous mesofilm (10 nm anatase TiO<sub>2</sub> nanopowder) is immersed in liquid, this film tends to absorb the surrounding liquid due to diffusion effect. The adsorbed amount of dye is normally affected by the immersion time and then this time must be accounted for. Once all the prepared films were coated with the same TiO<sub>2</sub> nanopowder at the same annealing temperature 723 K (450°C), the immersion time may be the uniquely influential factor to be analyzed at this stage since it is related to the dye concentration. Because of all the above conditions, the films that were immersed for 5.5 h yielded the highest efficiency. This may be attributed to the low adsorption rate of TiO<sub>2</sub> mesoporous film for approximately big size Ruthenium N719 dye. Over the first four hours, the film

has not yet adsorbed a sufficient dye amount. At the fifth hour, TiO<sub>2</sub> film reaches maximum adsorption relaxation capability, which led to highest sensitizing efficiency. With immersion time longer than 5.5 h, aggregation of dye molecules could possibly occur inside the porous film. This aggregation may quench the dye photoactivity, yielding low dye sensitizing and then low DSSC efficiency<sup>[22]</sup>.

As regards to TABLE 2, the DSSCs that give higher efficiencies are those used Ruthenium N719 dye and pomegranate juice. These two cells, when doped with AgNO<sub>3</sub>, experience higher short-circuit current, open-circuit voltage (V<sub>oc</sub>) and filling factor in comparison to that without additive. On the other hand, cells of other dyes showed unsystematic behavior because of their low output current and subsequently low efficiency. In general, adding AgNO<sub>3</sub> to all DSSCs resulted in various ratios of efficiency increase. Among all tested metallic additives, AgNO<sub>3</sub> was found as the best for efficiency enhancement. This may be due to its redox potential value which is relatively higher for ionic silver (-1.8 V NHE)<sup>[23]</sup>.

In the case of 5.5 hours immersion time and 5 × 10<sup>-4</sup> M Ruthenium N719 dye concentration 1 gm. / L of AgNO<sub>3</sub>, the DSSC efficiency was upgraded from 1.95 to 3.7 %. In addition, after having this concentration of AgNO<sub>3</sub> all the natural DSSC efficiencies were nearly doubled. It is commonly understood that the presence of small amounts of silver facilitates the absorbance of visible light according to multi-scattering mechanism.

Typical transmission spectra for different concentration of AgNO<sub>3</sub> additive are illustrated in Figure 7.

The spectra in this figure can justify that a cell with lower AgNO<sub>3</sub> concentration could exhibit transmittance higher than that of other cells and hence, such lower

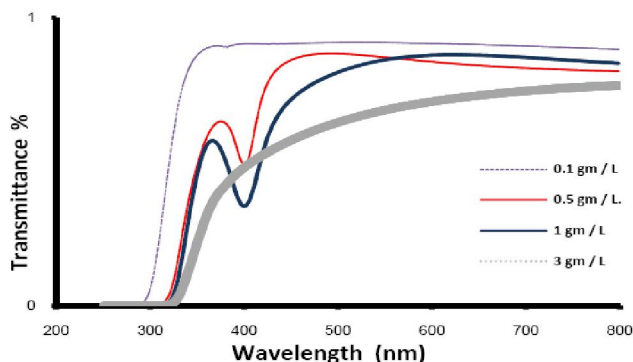
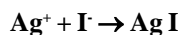


Figure 7 : Transmission spectra for DSSC at different AgNO<sub>3</sub> concentration

concentration has negligible scattering effect in this process. More obvious scattereffect could be observed with increasing AgNO<sub>3</sub> concentration leading to a subsequent reduction in transmittance. Further increase of AgNO<sub>3</sub> concentration resulted in a pronounced drop located at (415nm), corresponding to a surface plasmon resonance of silver which favors more electron excitation<sup>[24,25]</sup>.

As AgNO<sub>3</sub> concentration had been increased upto 3 gm /L), the transmittance was reduced to 50 % of its initial value. Moreover, silver possesses the ability to reduce recombination due to its trapping of excited electrons throughout the introduction of the Fermi level of silver which is located just below the conduction band of TiO<sub>2</sub><sup>[26]</sup>. In fact, AgNO<sub>3</sub> is relatively stable to light, i.e., the photoirradiation on the DSSC was not affected by AgNO<sub>3</sub> concentration<sup>[27]</sup>. There is an optimum concentration of AgNO<sub>3</sub> (1 gm. /L) which brings about better efficiency enhancement to the DSSC, Figure 5. With concentrations above and below this value, cell efficiency would be degraded. The dependence of cell efficiency upon the concentration of AgNO<sub>3</sub> may be justified as follows:

In the case of concentration lower than 1 gm. /L, a presence of Ag<sup>+</sup> cation could promote the electrolyte ability to carry the electrical charge as the Ag<sup>+</sup> concentration increased. Such mechanism gives rise to an efficiency enhancement towards a maximum value at a specific AgNO<sub>3</sub> concentration. On the other hand, more increase of AgNO<sub>3</sub> concentration above 1 gm. /L would lead to an efficiency reduction may be attributed to undesired possible chemical reaction. Since the utilized electrolyte mainly consists of Potassium iodide and iodide, which are halides, the excess of silver cation Ag<sup>+</sup>, may upsurge the silver ion reaction with halide sources to produce an insoluble yellow precipitate of silver iodide according to the halide abstraction reaction<sup>[28]</sup>.



This process will reduce amount of I<sup>-</sup> and distorts the optimum I<sup>-</sup>/I<sub>3</sub><sup>-</sup> ratio preventing the required dye regeneration. As this process proceeds, the sensitizing activity of the dye will be limited and then the DSSC efficiency will be decreased.

Results listed in TABLE 2 show that for chemically synthesized DSSC and upon adding AgNO<sub>3</sub>

## Full Paper

to the electrolyte, the short-circuit current and conversion efficiency are doubled with slight increase in the open-circuit voltage and fill factor. Alternatively, in natural DSSC this addition brings about doubling the fill factor, maximum circuit voltage and conversion efficiency keeping the circuit current unchanged. The characteristic features of natural DSSC may be due to the acidic environment (excess of  $H^+$ ) in the natural juice which compensate the iodide silver reaction.

### CONCLUSION

In conclusion, we have investigated the feasibility of using silver nitrate, as an enhancement additive in a DSSC. The results here focus only on two sensitizer dyes: natural pomegranate juice dye and organometallic dye N719.

As a result, the power conversion efficiency was nearly doubled after adding a 1 gm. /L  $AgNO_3$  to the electrolyte redox solution. This addition concentration could offer a viable low-cost alternative enhancement to conventional DSSC in both natural and organometallic dyes.

However, as the results reported in this work, long immersion time yields a great tendency for N719 to aggregate as it increases up to six hours.

### REFERENCES

- [1] I.Ahmad, U.Khan, Y.K.Gun'ko; *Mater.Chem.*, **21**, 16990-16996 (2011).
- [2] S.Ahmad, E.Guillén, L.Kavan, M.Grätzel, M.K.azeeruddin; *Energy Environ.Sci.*, **6**, 3439-3466 (2013).
- [3] B.O'Regan, M.Grätzel; *Nature*, **353**, 73 (1991).
- [4] M.Grätzel; *Nature*, **414**, 338 (2001).
- [5] Y.Chiba, A.Islam, Y.Watanabe, R.Komiya, N.Koide, L.Han; *Jpn. J.Appl.Phys.*, Part 2, **45**, 638 (2006).
- [6] M.K.Nazeeruddin, P.Pechy, M.Grätzel; *Chem.Commun.*, **18**, 1705-1706 (1997).
- [7] M.Grätzel; *Inorg.Chem.*, **44**(20), 6841-6851 (2005).
- [8] A.Hagfeldt, G.Boschloo, L.Sun, L.Kloo, H.Pettersson; *Chem.Rev.*, **110**, 6595-6663 (2010).
- [9] A.Hagfeldt, M.Grätzel; *Light-Induced Redox Reactions in Nanocrystalline Systems*, *Chem. Rev.*, **95**(1), 49-68 (1995).
- [10] N.Papageorgiou, W.F.Maier, M.Grätzel; *J.Electrochem.Soc.*, **144**(3), 876-884 (1997).
- [11] N.Papageorgiou; *CoorChem Rev.*, **248**, 1421 (2004).
- [12] N.Kato, K.Higuchi, H.Tanaka, J.Nakajima, T.Sano, T.Toyoda; *Solar Energy Materials and Solar Cells*, **95**(1), 301-305 (2011).
- [13] S.Nakade, T.Kanzaki, W.Kubo, T.Kitamura, Y.Wada, S.Yanagida; *J.Phys.Chem.B*, **109**, 3480-3487 (2005).
- [14] F.Fabregat-Santiago, J.Garcia-Canadas, E.Palomares, J.N.Clifford, S.A.Haque, J.R.Durrant, G.Garcia-Belmonte, J.Bisquert; *J.Appl.Phys.*, **96**, 6903-6907 (2004).
- [15] A.Alessandra, L.A.Naomi, M.J.Attila, D.Lynn, W.Pawel, O.L.David, S.Kenji, M.Shogo, S.Leone; *Energy Environ.Sci.*, **2**, 1069-1073 (2009).
- [16] F.Sauvage, S.Chhor, A.Marchioro, J.Moser, M.J.Grätzel; *Am.Chem.Soc.*, **133**, 13103-13109 (2011).
- [17] J.R.Jennings, Q.Wang; *J.Phys.Chem.C*, **114**, 1715-1724 (2010).
- [18] C.Zhang, Y.Huang, Z.Huo, S.Chen, S.J.Dai; *Phys.Chem.C*, **113**, 21779-21783 (2009).
- [19] R.Mori, T.Ueta, K.Sakai, Y.Niida, Y.Koshiba, L.Lei, K.Nakamae, Y.Ueda; *J Mater Sci.*, **46**(5), 1341-1350 (2011).
- [20] G.P.Smestad, M.Grätzel; *J.Chem.Educ.*, **75**(6), 752 (1998).
- [21] Y.Kim, H.Kang, Y.Jang, S.Lee, S.Lee, K.Jung, J.Lee, M.Kim; *Int. J.Mol.Sci.*, **9**, 2745-2756 (2008).
- [22] A.J.Al-Wattar, B.T.Chiad, W.A.A.Twej, S.S.Al-Awadi; *CEJP*, **4**, 341-348 (2006).
- [23] K.Mallick, M.Witcomb, M.Scurrall; *Mat.Chem.Phys.*, **97**, 283-287 (2006).
- [24] A.R.Malagutti, A.Mourao, R.Garbin, C.Ribeiro; *App.Cata. B: Env.*, **90**, 205-212 (2009).
- [25] M.K.Seery, R.George, P.Floris, S.C.Pillai; *J.Photochem.Photobiol. A*, **189**, 258-263 (2007).
- [26] C.Gunawan, W.Y.Teoh, C.P.Marquis; *J.Lifia, R.Amal,Small*, **5**(3), 341-344 (2009).
- [27] L.Cui, L.Baoxin; *Anal.and Bioanal.Chem.*, **401**(1), 229-235 (2011).
- [28] D.N.Bose, P.A.Govindacharyulu; *Bull.of Mater.Sci.*, **2**(4), 221-231 (1980).